# Unsteady Aerodynamic Response Modeling: A Parameter-Varying Approach

Maziar S. Hemati,[*] Scott T. M. Dawson, [†]
and Clarence W. Rowley [‡]

*Mechanical and Aerospace Engineering, Princeton University, Princeton, NJ 08544*

**Current low-dimensional aerodynamic modeling capabilities are greatly challenged in the face of aggressive flight maneuvers, such as rapid pitching motions that lead to aerodynamic stall. Nonlinearities associated with leading-edge vortex development and flow separation push existing real-time-capable aerodynamics models beyond their predictive limits. The inability to accurately predict the aerodynamic response of an aircraft to sharp maneuvers makes flight simulation for pilot training unrealistic and, thus, ineffective at adequately preparing pilots to safely handle compromising flight scenarios. Inaccurate low-dimensional models also put practical approaches for aerodynamic optimization and control out of reach. In the present development, we make a push toward realizing real-time-capable models with enhanced predictive performance for flight operations by considering the simpler problem of modeling an aggressively pitching airfoil in a low-dimensional manner. We propose a parameter-varying model, composed of three coupled quasi-linear sub-models, to approximate the response of an airfoil to arbitrarily prescribed aggressive ramp-hold pitching kinematics. An output error minimization strategy is used to identify the low-dimensional quasi-linear parameter-varying sub-models from input-output data gathered from low-Reynolds number (Re = 100) direct numerical fluid dynamics simulations. The resulting models have noteworthy predictive capabilities for arbitrary ramp-hold pitching maneuvers spanning a broad range of operating points, thus making the models especially useful for aerodynamic optimization and real-time control and simulation.**

## Nomenclature

| | |
|---|---|
| $\alpha$ | Angle of attack, or pitch angle |
| $\dot{\alpha}$ | Pitch rate |
| $\ddot{\alpha}$ | Pitch angular acceleration |
| $\epsilon_{\text{rms}}$ | Root mean square error with respect to simulated output data |
| $\boldsymbol{\xi}$ | Optimization parameter for model identification |
| $\rho$ | Fluid density |
| $(\mathcal{A}, \mathcal{B}, \mathcal{C}, \mathcal{D})$ | Full parameter-varying state-space system |
| $(\tilde{A}, \tilde{B}, \tilde{C}, \tilde{D})$ | Linear parameter varying sub-model state-space system |
| $c$ | Chord length |
| $C_d, C_l, C_m$ | Drag, lift, and pitching moment coefficients |
| $C_{d,\alpha=0°}, C_{l,\alpha=0°}, C_{m,\alpha=0°}$ | Nominal drag, lift, and pitching moment at $\alpha = 0°$ |
| $\mathbf{p}$ | Linear parameter-varying model parameter/pseudo-input vector |
| $t^*$ | Convective time, $Ut/c$ |

---
[*]Post-Doctoral Research Associate, Mechanical and Aerospace Engineering, Princeton University, AIAA Member.
[†]Graduate Student, Mechanical and Aerospace Engineering, Princeton University, AIAA Student Member
[‡]Professor, Mechanical and Aerospace Engineering, Princeton University, AIAA Associate Fellow

American Institute of Aeronautics and Astronautics

| | |
|---|---|
| $\mathbf{u}$ | Linear parameter-varying model input vector |
| $U$ | Free stream fluid speed |
| $\tilde{\mathbf{x}}$ | Identified internal model state |
| $\mathbf{x}$ | Total aerodynamic state vector, $(\tilde{\mathbf{x}}, \mathbf{p})$ |
| $\mathbf{y}$ | Output vector $(C_l, C_d, C_m)$ of forces and moments |
| $y^i, y$ | Sub-model force/moment output, $i \in (C_l, C_d, C_m)$ |
| $y^{\text{train}}$ | Training maneuver simulated force/moment output data |

## I.  Introduction

Agile flight maneuvers are tightly coupled with unsteady aerodynamic effects; body motions lead to vortex shedding, while the velocities induced by shed vortices lead to aerodynamic body forcing. Numerous low-dimensional models have been developed to characterize these unsteady aerodynamic processes, most notably motivated by progress in biologically inspired flight systems. The ability to model the force response of a flight vehicle to unsteady motions, in a computationally efficient manner, is essential for real-time flight simulation, control, and optimization. Unfortunately, current approaches to low-dimensional unsteady aerodynamic modeling yield inadequate predictions when faced with aggressive flight maneuvers that move an air-vehicle through many operating regimes characterized by appreciably different wake vortex interactions. This is problematic, for example, in the realm of flight simulation for pilot training, where realistic models are needed to adequately train pilots to effectively manage compromising flight scenarios (e.g., sharp wind gusts and aerodynamic stall). Accuracy and reliability of low-dimensional models over a broad operating range also plays a major role in aerodynamic optimization, since the topology of a given cost function inherently depends on the specific dynamical model used.

Work on unsteady aerodynamic modeling is long-standing and consistently improving. Numerous models, grounded in fundamental aerodynamic principles, have continued to expand aerodynamic predictive capabilities to progressively more ambitious situations. Beginning in the 1920s and 1930s, Wagner and Theodorsen developed elegant models that relied upon a decomposition of the aerodynamic force response into contributions from circulatory (i.e., vortex induced) and non-circulatory (i.e., added mass) components.[1,2] To extend this general framework to a broader range of aerodynamic maneuvers, numerous models have been developed since then, based on various vortex representations such as vortex sheets,[3,4,5,6,7,8] continuous sequences of point vortices,[9,10,11,12] and finite sets of point vortices with evolving strengths.[13,14,15,16,17] Most vortex models are able to predict forces and moments with remarkable accuracy over a wide range of kinematics because they account for the most relevant parameters that influence the aerodynamic response (i.e., the evolving distribution of vorticity in the flow). Unfortunately, owing to their large dimensionality, the models that exhibit superb predictive capabilities are too computationally costly to be used in real-time. On the other hand, the models that are suitable for real-time implementation lack sufficient accuracy to be effective in many applications.

To this end, a multitude of aerodynamic modeling approaches have invoked the data-driven paradigm of dynamical systems theory to identify low-dimensional computationally efficient models for real-time utilization. Data-driven methods are often desirable because they work with empirical aerodynamic input-output response data directly, thus allowing a low-order model to be "trained" on a representation of the dynamics it is intended to reproduce. Recently, the eigensystem realization algorithm (ERA), a data-driven method, was used to construct linear state-space models of an airfoil undergoing pitch, plunge, and surge maneuvers.[18,19] The models realized from the ERA approach proved successful in conjunction with $\mathcal{H}_\infty$ control methods—which are robust to model uncertainty—for tracking commanded lift trajectories. However, the models demonstrated inadequate predictive capabilities, for the purpose of realistic flight simulation and aerodynamic optimization, when subjected to dynamics that moved away from the operating points about which the models were designed.

Gain scheduling between sets of linear models, such as ERA models, has been proposed as a means of resolving the shortcomings of local linear state-space representations. The approach of gain-scheduling between linear models has been used successfully in various application areas, including aircraft flight control;[20,21,22] however, the framework is not without drawbacks. For example, it is often the case that a large collection of linear models and slow variations between operating points is required to satisfy controller performance specifications,[23] thus making the framework ill-suited for aggressive aerodynamic maneuvers,

where variations between operating points is, by definition, rapid.

In response to the limitations associated with gain scheduling between linear models, much research has focused on linear parameter-varying (LPV) systems, where the system matrices are known functions of a measurable set of time-varying parameters. Gain-scheduled controller design within the LPV framework allows for tighter performance bounds and can deal with fast variations of the operating point.[24] The LPV framework has been applied successfully to the modeling and control of various aircraft systems,[25, 26, 27] but much of this work has focused on variations in Reynolds and Mach numbers; progress on LPV methods for aggressive flight maneuvers remains underdeveloped.

In the present manuscript, we study the viability of using parameter-varying models for accurately predicting force and moment responses to aggressive aerodynamic maneuvers. Encouraged by observations reported in Hemati (2013) and Hemati et al. (2014)—that empirical force response data of an unsteady airfoil, with both leading and trailing edge vortex shedding, can be accurately reproduced, over a short time window, by a small set of vortex parameters (i.e., the position and strength of two point vortices)[28, 29]—we devise a parameter-varying model that uses the angle of attack $\alpha$ and its associated rate of change $\dot{\alpha}$ as proxies for the pertinent vortex parameters influencing the force and moment response to rapid pitching motions. We propose a model structure in the form of three quasi-LPV (qLPV) sub-systems—LPV systems whose scheduling parameters include a subset of the states[22, 26]—and invoke an output-error minimization procedure to identify the sub-models from empirical aerodynamic force and moment response data generated in direct numerical fluids simulations. Motivated by our desire to better understand the principles that govern the aerodynamics of unsteady flight, we restrict our attention to idealized geometries and simple motions. Specifically, we study the response of a flat plate airfoil to aggressive pitching kinematics. The pitching maneuvers are fully prescribed (i.e., no effort is made to include flight dynamics effects in the system), and the free-stream velocity remains fixed at all times, such that the pitch angle $\theta$ and the angle of attack $\alpha$ are equivalent throughout a maneuver. The resulting qLPV models yield respectable predictive capabilities for lift, drag, and pitching moment over a broad range of operation (i.e., $|\alpha| \leq 25^\circ$), testifying to the promise of parameter-varying representations in the context of aggressive aerodynamic response modeling.

We begin by discussing the general notion of parameter-varying models in an aerodynamic context followed, in Section II, by a development of the qLPV model structure used to represent the lift, drag, and pitching moment response to commanded pitch accelerations $\ddot{\alpha}$. Section III introduces and develops the system identification method used for realizing qLPV models from input-output data, while details pertaining to the generation of aerodynamic input-output data for model identification are presented in Section IV. In Section V, force and moment predictions from the identified qLPV model are compared with results from direct numerical simulations over a variety of operating regimes; the qLPV model is also compared with an ERA lift response model in an effort to highlight the advantages of parameter-varying models over linear models in the context of unsteady aerodynamic response modeling.

## II.  Pitching Airfoil Parameter-Varying Model Formulation

The aim of the present study is to use empirical input-output data, measured from either numerical simulations or physical experiments, to identify a low-order model that accurately represents the dynamical lift ($C_l$), drag ($C_d$), and pitching moment ($C_m$) response of an airfoil to arbitrary pitching maneuvers. In an effort to better ascertain a fundamental understanding with regards to modeling, we restrict our attention to a flat-plate airfoil undergoing fully-prescribed pitching motions about its quarter-chord point, as depicted in Figure 1. Additionally, we enforce that the free-stream velocity $U$ remains constant throughout a maneuver such that the angle of attack $\alpha$ and the pitch angle $\theta$ are equivalent. We also take $\ddot{\alpha}$, the angular acceleration about the pitch axis, as the system input, since pitching maneuvers of physical interest can be generated from this choice.

To be of any use in effectively modeling aggressive pitch maneuvers, the identified model must be able to approximate the response of the airfoil to strong variations in the relevant flow states. For simplicity, we make a particular choice to use the angle of attack and its rate of change $(\alpha, \dot{\alpha})$ as proxies for the aerodynamic states that may be more pertinent to the overall dynamics, but are either difficult to measure directly or challenging to represent adequately in a low-dimensional manner (e.g., vorticity distribution, as depicted in Figure 2). Our choice to parameterize the airfoil response via the state of the airfoil $(\alpha, \dot{\alpha})$ is a reasonable one, since the state of the fluid varies significantly based on the angle of attack and the pitch rate; as highlighted in Figure 2, there is significant contrast between the flow state for different angles of
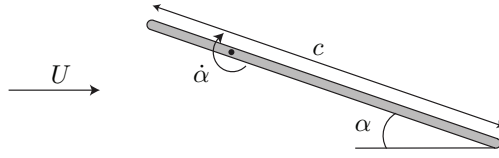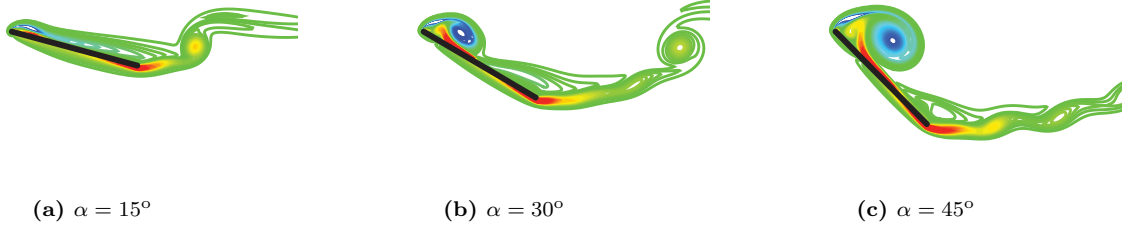
**Figure 1:** Pitching airfoil study-configuration. We restrict our attention to the response of a flat-plate airfoil undergoing fully-prescribed pitching kinematics about its quarter-chord point. Moreover, we maintain a constant free-stream velocity $U$ such that the angle of attack $\alpha$ and pitch angle $\theta$ are equivalent to one another throughout a maneuver.

attack at a fixed pitch rate and for different pitch rates at a given angle of attack. Since we know that the airfoil state evolves by means of a double integrator with respect to the input,

$$\begin{bmatrix} \alpha_{k+1} \\ \dot{\alpha}_{k+1} \end{bmatrix} = \begin{bmatrix} 1 & \Delta t \\ 0 & 1 \end{bmatrix} \begin{bmatrix} \alpha_k \\ \dot{\alpha}_k \end{bmatrix} + \begin{bmatrix} \Delta t^2/2 \\ \Delta t \end{bmatrix} \ddot{\alpha}_k, \tag{1}$$

these parameters are readily available and, therefore, a convenient choice from a modeling standpoint. Here, we have expressed the evolution of the airfoil state from time $t_k$ to time $t_{k+1}$ by means of its discrete-time state-space representation, where $\Delta t = t_{k+1} - t_k$.

$$K = 0.2$$



**(a)** $\alpha = 15°$        **(b)** $\alpha = 30°$        **(c)** $\alpha = 45°$

$$K = 0.7$$



**(d)** $\alpha = 15°$        **(e)** $\alpha = 30°$        **(f)** $\alpha = 45°$
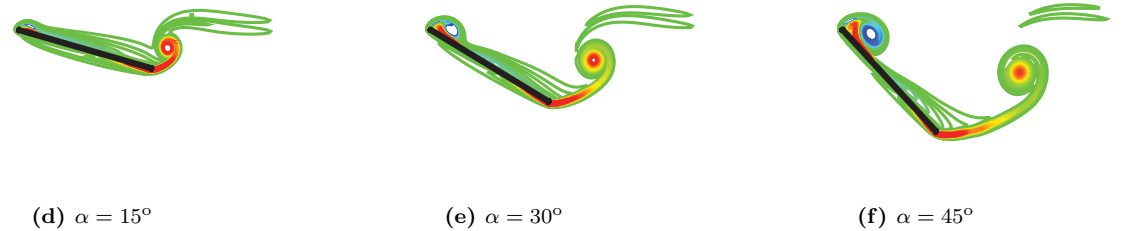
**Figure 2:** The state of the fluid varies significantly with the state of the airfoil $(\alpha, \dot{\alpha})$. Here, we visualize snapshots of the vorticity-field associated with a canonical pitch-up maneuver of a flat-plate rotating about its leading-edge for (a,d) $\alpha = 15°$, (b,e) $\alpha = 30°$, and (c,f) $\alpha = 45°$ at reduced frequencies of $K = 0.2$ (top row) and $K = 0.7$ (bottom row), where $K := \dot{\alpha}c/(2U)$. The parameter-varying models of the present study make use of $(\alpha_k, \dot{\alpha}_k)$ as proxies for the dominant flow structures, augmented by a set of evolving internal states essential for modeling the dynamics of any unaccounted flow physics. Figure adapted from Hemati et al. (2014).

In addition to our particular choice to set $(\alpha_k, \dot{\alpha}_k)$ as parameters, we also include a set of internal states $\tilde{\mathbf{x}}_k$ in order to model the time-evolution of any unaccounted flow physics. Based on these choices, the general dynamical system that maps from angular acceleration inputs $\ddot{\alpha}_k$ to a column vector of force and moment

American Institute of Aeronautics and Astronautics

outputs $\mathbf{y}_k = (C_{l_k}, C_{d_k}, C_{m_k}) \in \mathbb{R}^3$ can be expressed as,

$$\mathbf{x}_{k+1} = \mathcal{A}(\alpha_k, \dot{\alpha}_k)\mathbf{x}_k + \mathcal{B}(\alpha_k, \dot{\alpha}_k)\ddot{\alpha}_k \tag{2a}$$

$$\mathbf{y}_k = \mathcal{C}(\alpha_k, \dot{\alpha}_k)\mathbf{x}_k + \mathcal{D}(\alpha_k, \dot{\alpha}_k)\ddot{\alpha}_k, \tag{2b}$$

where the *total aerodynamic state* $\mathbf{x}_k := (\tilde{\mathbf{x}}_k, \dot{\alpha}_k, \alpha_k) \in \mathbb{R}^n$ is a column vector composed of the *airfoil states* $(\alpha_k, \dot{\alpha}_k)$ and a set of yet to be identified *internal states* $\tilde{\mathbf{x}}_k \in \mathbb{R}^{n-2}$. By parameterizing the system dynamics by means of the airfoil states, which are also included in the total aerodynamic state vector $\mathbf{x}_k$, the system evolution takes the form of a quasi-linear parameter-varying (qLPV) system—an LPV system for which the parameters correspond to a subset of the system states.[22, 26]

The goal of the identification problem is to approximate $(\mathcal{A}, \mathcal{B}, \mathcal{C}, \mathcal{D})$ from input-output data measured during a training maneuver, such that the model in (2) robustly captures the dynamical response to arbitrary "untrained" maneuvers. Rather than setting out to identify the full model in (2) from a single invocation of a system identification procedure, we decompose the problem into three separate single-input single-output (SISO) parameter-varying systems in order to make the identification procedure (discussed in Section III) more manageable. Such a decomposition allows the individual sub-models to be coupled to one another; thus, the full model is able to maintain important dynamical interplays, between the simplified SISO sub-models, that may be necessary for accurate prediction (e.g., the drag sub-model requires an additional parameterization by the lift coefficient predicted by the lift sub-model in order to yield reliable predictions, as will be discussed in Section V). Upon identifying these individual systems, we can combine the identified models to construct the full system model (2), a schematic of which is presented in Figure 3.
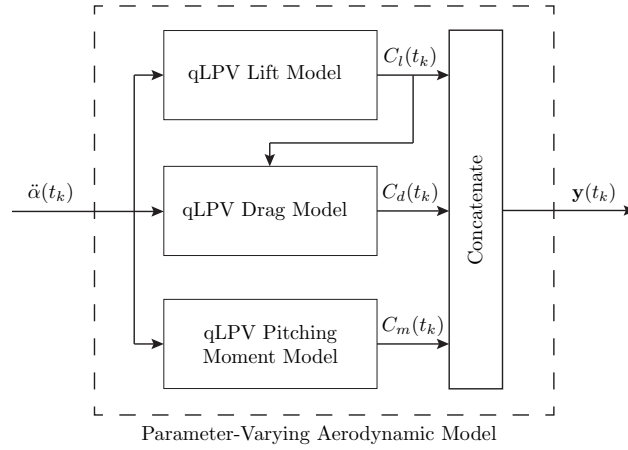


**Figure 3:** Decomposition of the parameter-varying aerodynamic model into three qLPV sub-models for system identification.

In addition to decoupling the full system model into three SISO sub-models, we further simplify the system identification task by assuming that each of these sub-models has affine parameter dependence. In doing so, we arrive at a set of qLPV sub-systems (i.e., LPV systems parameterized by a subset of the system states), for which the state-space representation of sub-system $i \in \{C_l, C_d, C_m\}$ can be expressed as,

$$\mathbf{x}_{k+1}^i = \mathcal{A}^i(\alpha_k, \dot{\alpha}_k)\mathbf{x}_k^i + \mathcal{B}^i(\alpha_k, \dot{\alpha}_k)\ddot{\alpha}_k \tag{3a}$$

$$y_k^i = \mathcal{C}^i(\alpha_k, \dot{\alpha}_k)\mathbf{x}_k^i + \mathcal{D}^i(\alpha_k, \dot{\alpha}_k)\ddot{\alpha}_k \tag{3b}$$

where

$$\mathcal{A}^i(\alpha_k, \dot{\alpha}_k) = A_0^i + A_\alpha^i \alpha_k + A_{\dot{\alpha}}^i \dot{\alpha}_k, \tag{3c}$$

$$\mathcal{B}^i(\alpha_k, \dot{\alpha}_k) = B_0^i + B_\alpha^i \alpha_k + B_{\dot{\alpha}}^i \dot{\alpha}_k, \tag{3d}$$

$$\mathcal{C}^i(\alpha_k, \dot{\alpha}_k) = C_0^i + C_\alpha^i \alpha_k + C_{\dot{\alpha}}^i \dot{\alpha}_k, \tag{3e}$$

$$\mathcal{D}^i(\alpha_k, \dot{\alpha}_k) = D_0^i + D_\alpha^i \alpha_k + D_{\dot{\alpha}}^i \dot{\alpha}_k, \tag{3f}$$

which is simply a weighted sum of several linear models with $(\alpha_k, \dot{\alpha}_k)$ serving as weights. The qLPV form is convenient because existing algorithms from LPV system identification theory can be invoked (with little

modification) to determine the system matrices $\mathcal{A}^i(\alpha_k, \dot{\alpha}_k)$, $\mathcal{B}^i(\alpha_k, \dot{\alpha}_k)$, $\mathcal{C}^i(\alpha_k, \dot{\alpha}_k)$, and $\mathcal{D}^i(\alpha_k, \dot{\alpha}_k)$, as will be shown in Section III. For a given set of parameters, this model reduces to a locally linear state-space model, which is typical of LPV and qLPV systems.[30] Although the qLPV model in (3) is similar is to a gain scheduled model (i.e., one that interpolates between a collection of linear models), it is not restricted to slow variations in the scheduling parameters;[23, 24] thus, the system model in (3) is well-suited for predicting the response to aggressive pitching maneuvers characterized by rapid variations in $(\alpha_k, \dot{\alpha}_k)$. For notational convenience, in the remainder, we will drop the superscript $i$ corresponding to each sub-model, keeping in mind that future developments are based on the definitions of inputs, parameters, outputs, and states that vary between sub-models.

Special considerations must be made for modeling the drag response; we acknowledge that the absence of a nonlinear coupling term in the drag model leaves much of the relevant dynamical behavior unmodeled. Numerical experiments indicate that including $C_l$ as a parameter in the drag sub-model substantially improves drag response predictions (c.f., Section V for further discussion). As such, we include a nonlinear coupling term by including the output of the lift sub-model $C_{l_k}$ as a model parameter in the qLPV drag sub-model, as shown in Figure 3. Thus, the qLPV drag sub-model has dynamics expressed by,

$$
\begin{align}
\mathbf{x}_{k+1} &= \mathcal{A}(\alpha_k, \dot{\alpha}_k, C_{l_k})\mathbf{x}_k + \mathcal{B}(\alpha_k, \dot{\alpha}_k, C_{l_k})\ddot{\alpha}_k \tag{4a} \\
y_k &= \mathcal{C}(\alpha_k, \dot{\alpha}_k, C_{l_k})\mathbf{x}_k + \mathcal{D}(\alpha_k, \dot{\alpha}_k, C_{l_k})\ddot{\alpha}_k \tag{4b}
\end{align}
$$

where

$$
\begin{align}
\mathcal{A}(\alpha_k, \dot{\alpha}_k, C_{l_k}) &= A_0 + A_\alpha \alpha_k + A_{\dot{\alpha}} \dot{\alpha}_k + A_{C_l} C_{l_k}, \tag{4c} \\
\mathcal{B}(\alpha_k, \dot{\alpha}_k, C_{l_k}) &= B_0 + B_\alpha \alpha_k + B_{\dot{\alpha}} \dot{\alpha}_k + B_{C_l} C_{l_k}, \tag{4d} \\
\mathcal{C}(\alpha_k, \dot{\alpha}_k, C_{l_k}) &= C_0 + C_\alpha \alpha_k + C_{\dot{\alpha}} \dot{\alpha}_k + C_{C_l} C_{l_k}, \tag{4e} \\
\mathcal{D}(\alpha_k, \dot{\alpha}_k, C_{l_k}) &= D_0 + D_\alpha \alpha_k + D_{\dot{\alpha}} \dot{\alpha}_k + D_{C_l} C_{l_k}. \tag{4f}
\end{align}
$$

Modeling the nonlinear coupling in this manner does not hinder our ability to invoke existing algorithms for identifying systems with affine parameter dependence, since we have chosen to decompose the full aerodynamic response model into three SISO sub-systems. That is, we can perform the identification procedure on the drag model independent of the lift model; $C_l$ now serves a measurable parameter in the drag sub-model, thus keeping the modeled drag response in the qLPV form required for the system identification methods presented in Section III.

## III.   Quasi-LPV Model Identification

Our ultimate goal is to determine an approximate dynamical representation for the aerodynamic pitching response of an airfoil from available input-output data such that the resulting model adequately reproduces the true system dynamics. As discussed in Section II, we anticipate that $(\alpha_k, \dot{\alpha}_k)$ will serve as suitable proxies for the state of the surrounding fluid during airfoil pitching motions. Furthermore, we expect that $(\alpha_k, \dot{\alpha}_k)$, together with a set of appropriately identified internal states that model the dynamical evolution of any remaining flow physics, will provide an adequate template for computing aerodynamic response models from input-output data.

Since the evolution equations corresponding to the airfoil states are already known (i.e., Equation (1)), we can recast the qLPV model into LPV form by relaxing the definitions of inputs and states for the purpose of system identification. Doing so is beneficial because the quasi-linear terms—i.e., the quadratic and bilinear terms arising from the fact that $(\alpha, \dot{\alpha})$ are included both as model states and model parameters—can be treated as known inputs to the system. Furthermore, such a rearrangement allows existing techniques for LPV system identification to be applied for qLPV system identification. Once the LPV representation is identified, the original qLPV form desired can be obtained through reversing the rearrangement procedure, which amounts to a simple exercise in accounting. We emphasize that such rearrangements are allowed because we know the evolution of the system parameters, given by (1), *a priori*; hence, we can compute a sequence of *pseudo-inputs* $\mathbf{p}_k := (\alpha_k, \dot{\alpha}_k) \in \mathbb{R}^2$, or in the case of the drag sub-model $\mathbf{p}_k := (\alpha_k, \dot{\alpha}_k, C_{l_k}) \in \mathbb{R}^3$, to be used during the identification step. We then move $\mathbf{p}_k$ from the total state vector $\mathbf{x}_k$ to the augmented input vector $\mathbf{u}_k := (\ddot{\alpha}_k, \mathbf{p}_k)$, leaving only the identified internal state $\tilde{\mathbf{x}}_k$ to serve as a state vector during model identification. In other words, we perform system identification on the LPV representation of the

system,

$$\tilde{\mathbf{x}}_{k+1} = \tilde{\mathcal{A}}(\mathbf{p}_k)\tilde{\mathbf{x}}_k + \tilde{\mathcal{B}}(\mathbf{p}_k)\mathbf{u}_k \qquad (5a)$$
$$y_k = \tilde{\mathcal{C}}(\mathbf{p}_k)\tilde{\mathbf{x}}_k + \tilde{\mathcal{D}}(\mathbf{p}_k)\mathbf{u}_k, \qquad (5b)$$

where the LPV system matrices $(\tilde{\mathcal{A}}, \tilde{\mathcal{B}}, \tilde{\mathcal{C}}, \tilde{\mathcal{D}})$ relate back to the qLPV system matrices $(\mathcal{A}, \mathcal{B}, \mathcal{C}, \mathcal{D})$ through a rearrangement of columns corresponding to the elements of $\mathbf{p}_k$ between the two representations. In this form, the quadratic and bilinear terms associated with the airfoil states (i.e., the quasi-linear terms) are treated as inputs, which are fully known; as such, the representation in (5) corresponds to an LPV model, which can be identified by means of output-error minimization techniques.

The objective of the system identification procedure adopted here is to determine, for each sub-model, a set of system matrices $(\tilde{\mathcal{A}}, \tilde{\mathcal{B}}, \tilde{\mathcal{C}}, \tilde{\mathcal{D}})$ that minimizes the output-error with respect to the training output data $y_k^{\text{train}}$, given the training input data $u_k$ (c.f., Section IV). We express this as a constrained minimization problem that uses the elements of the LPV system matrices, $\boldsymbol{\xi} := (\tilde{\mathcal{A}}, \tilde{\mathcal{B}}, \tilde{\mathcal{C}}, \tilde{\mathcal{D}})$, as optimization parameters,

$$\min_{\boldsymbol{\xi}} \quad J(\boldsymbol{\xi}) \quad := \quad \sum_{k=1}^{N} \|y_k^{\text{train}} - y_k(\boldsymbol{\xi})\|_2^2 \qquad (6a)$$
$$\text{such that} \quad \tilde{\mathbf{x}}_{k+1}(\boldsymbol{\xi}) = \tilde{\mathcal{A}}(\mathbf{p}_k)\tilde{\mathbf{x}}_k(\boldsymbol{\xi}) + \tilde{\mathcal{B}}(\mathbf{p}_k)\mathbf{u}_k \qquad (6b)$$
$$y_k(\boldsymbol{\xi}) = \tilde{\mathcal{C}}(\mathbf{p}_k)\tilde{\mathbf{x}}_k(\boldsymbol{\xi}) + \tilde{\mathcal{D}}(\mathbf{p}_k)\mathbf{u}_k, \qquad (6c)$$

where $y_k(\boldsymbol{\xi})$ is the model-predicted output, which is determined from the model associated with $\boldsymbol{\xi}$.

Although we can compute a minimizing solution to this constrained nonlinear and non-convex optimization problem via gradient descent methods (e.g., Levenberg-Marquardt[31] in the present study), two additional challenges must be addressed beforehand. First, the non-uniqueness of a state-space realization introduces further complexity when determining the descent directions in the optimization algorithm; care must be taken to exclude descent directions for which the cost function does not change, since these solutions will yield the same input-output behavior.[32,33] In the present work, we invoke the method proposed by Lee and Poolla (1997) and extended to the LPV output-error minimization problem by Verdult and Verhaegen (2001) to exclude such descent directions during the gradient descent iterations. Second, the optimization problem is further complicated by the presence of multiple local minima, many of which are associated with models that yield unsatisfactory predictive performance for maneuvers that deviate from the training maneuver. Numerical solutions of the optimization problem are very sensitive to the initial model iterate. As such, we follow the subspace method of Verdult and Verhaegen (2001), which relies on approximate dynamical relations between various terms in the LPV system, to determine an initial model iterate for the gradient search algorithm; this general approach has been shown to lead to initial model guesses suitable for the output-error minimization problem in a variety of contexts.[24] Here, a kernel formulation is implemented to yield solutions to the subspace identification problem in a computationally tractable manner.[34] We note that subspace methods can also be used to give an indication of the appropriate dimension to impose on the identified internal state $\tilde{\mathbf{x}}_k \in \mathbb{R}^{n-2}$, thus guiding our choice in the selection of dimensions for the system matrices. In the present study, the LPV system identification computations discussed above are performed using the BILLPV Toolbox, v2.2.[35]

## IV.  Aerodynamic Input-Output Training Data

Now that we have proposed a parameter-varying representation for the aerodynamic response of a pitching airfoil and determined a means of identifying the specific qLPV sub-models that comprise it, we are left with the final step of providing suitable input-output data for model identification. In an effort to provide sufficiently rich frequency content in the training maneuver, we generate input-output response data associated with a flat-plate undergoing fully-prescribed sequences of pseudo-random ramp-hold pitching kinematics (i.e., no effort is made to include flight dynamics effects in the system). The pseudo-random ramp-hold maneuver in $\alpha$ arises by twice integrating a sequence of pulse inputs—pseudo-random in magnitude, pulse-width, and frequency—in $\ddot{\alpha}$, as in (1). Moreover, the imposed maneuvers are simulated such that the free-stream velocity $U$ remains fixed at all times, and the pitch angle $\theta$ and the angle of attack $\alpha$ are equivalent throughout a maneuver. These maneuvers have been considered previously in the context of ERA-based pitching airfoil models by Brunton et al. (2013) and Brunton et al. (2014).[18,19] Additionally, in the present development,

we compute the aerodynamic response of a flat-plate airfoil, pitching about its quarter-chord (c.f., Figure 1), by means of an immersed boundary projection method (IBPM)[36,37] at Re = 100; this was also the technique used by Brunton et al. (2013) and Brunton et al. (2014), thus providing a reasonable baseline for comparing identified qLPV models with identified ERA models.[18,19] The specific training maneuver used for model identification in this study is shown in Figure 4. The aerodynamic forces and moments are non-dimensionalized by $\rho U^2 c/2$ and $\rho U^2 c^2/2$, respectively, where $\rho$ is the fluid density and $c$ is the length of the chord.

Finally, we note that the force/moment training data must be preprocessed such that the steady-state $\alpha = 0^\circ$ baseline value is removed from each signal prior to performing system identification. In other words, the identification is performed on $(C_l - C_{l,\alpha=0^\circ})$, $(C_d - C_{d,\alpha=0^\circ})$, and $(C_m - C_{m,\alpha=0^\circ})$, with the steady-state $\alpha = 0^\circ$ contribution re-introduced as a constant term in the output equation. In the present work, we only need to account for this contribution in the drag equations, since the steady-state lift and pitching moment are zero for a flat-plate at $\alpha = 0^\circ$.

## V.  Quasi-LPV Pitching Model Results and Discussion

In the present section, we set out to identify a qLPV realization for airfoil pitching dynamics using the output-minimization approach described in Section III. To do so, we begin with the simulated force and moment response of the airfoil to the prescribed pseudo-random ramp-hold pitching maneuver shown in Figure 4. The identified sub-models capture the dynamical response to lift, drag, and pitching moment over 60 convective time units to within a root-mean-squared error $\epsilon_{\rm rms} \sim \mathcal{O}(10^{-2})$ or better. In order to demonstrate the validity of the model, we use the qLPV realization identified from the maneuver in Figure 4 to predict the dynamical response to several "untrained" maneuvers over 50 convective time units and with differing $|\alpha|$ bounds.

Predictions from the identified lift sub-model are favorable across all of the untrained pitching maneuvers with $|\alpha| \leq 25^\circ$ that were considered, as presented in Figure 5. In fact, the identified parameter-varying model yields predictions with consistent levels of error across all regimes: (a) $\epsilon_{\rm rms}^{\rm LPV} = 3.7 \times 10^{-3}$ at $|\alpha| \leq 5^\circ$, (b) $\epsilon_{\rm rms}^{\rm LPV} = 2.1 \times 10^{-2}$ at $|\alpha| \leq 15^\circ$, and (c) $\epsilon_{\rm rms}^{\rm LPV} = 6.5 \times 10^{-2}$ at $|\alpha| \leq 25^\circ$. An ERA model, identified as in Brunton et al. (2014) from impulse response simulations beginning from $\alpha = 0^\circ$, exhibits diminishing predictive accuracy with increased pitch amplitude: (a) $\epsilon_{\rm rms}^{\rm ERA} = 1.5 \times 10^{-2}$ at $|\alpha| \leq 5^\circ$, (b) $\epsilon_{\rm rms}^{\rm ERA} = 2.8 \times 10^{-2}$ at $|\alpha| \leq 15^\circ$, and (c) $\epsilon_{\rm rms}^{\rm ERA} = 1.4 \times 10^{-1}$ at $|\alpha| \leq 25^\circ$. This comparison demonstrates the superiority of a parameter-varying model over a single linear model in predicting the unsteady aerodynamic response to maneuvers performed at both small and large angles of attack.

The drag model performs similarly (c.f., Figure 6), with (a) $\epsilon_{\rm rms}^{\rm LPV} = 4.3 \times 10^{-3}$ at $|\alpha| \leq 5^\circ$, (b) $\epsilon_{\rm rms}^{\rm LPV} = 4.9 \times 10^{-3}$ at $|\alpha| \leq 15^\circ$, and (c) $\epsilon_{\rm rms}^{\rm LPV} = 1.6 \times 10^{-2}$ at $|\alpha| \leq 25^\circ$. However, we note that this is only the case when $C_l$ is included as a parameter in the drag sub-model, as parameterization by $(\alpha, \dot{\alpha})$ alone is not sufficient for reliable drag predictions. A crude explanation for this relates back to the steady-state drag curve, which is a nonlinear function of the angle of attack. Since, in the case of a flat-plate, the drag for $\pm\alpha$ are indistinguishable from one another, a linear model based on $\alpha$ alone will be a poor approximation. Although we can improve the approximation by introducing $|\alpha|$, $\sin\alpha$, and other nonlinear parameterizations, numerical experiments indicate that the explanation above is incomplete. We find that introducing $C_l$ as a parameter leads to orders of magnitude improvement in the model's predictive performance, which may be attributed to the close relationship between $C_l$ and the bound circulation of the airfoil; that is, $C_l$ may improve the predictions because it serves as a proxy for circulatory contributions to the drag.

Finally, the pitching moment sub-model also demonstrates consistent performance across all three maneuvers (c.f., Figure 7): (a) $\epsilon_{\rm rms}^{\rm LPV} = 8.5 \times 10^{-4}$ at $|\alpha| \leq 5^\circ$, (b) $\epsilon_{\rm rms}^{\rm LPV} = 2.8 \times 10^{-3}$ at $|\alpha| \leq 15^\circ$, and (c) $\epsilon_{\rm rms}^{\rm LPV} = 4.3 \times 10^{-3}$ at $|\alpha| \leq 25^\circ$.

Despite the promising predictive performance demonstrated by the identified parameter-varying model for ramp-hold pitch maneuvers with $|\alpha| \leq 25^\circ$, the framework based on $(\alpha, \dot{\alpha})$ quickly deteriorates for $|\alpha|$ beyond approximately $30^\circ$. This observation indicates that for larger angles of attack, $(\alpha, \dot{\alpha})$ alone is not an adequately rich set of proxy parameters for the relevant fluid flow physics. In order to reliably predict and model the unsteady aerodynamic response at larger angles of attack, a parameter-varying approach will necessarily require additional parameters to either augment or replace the set $(\alpha, \dot{\alpha})$. Viable candidates are expected to relate back to pertinent flow qualities, such as the evolving vorticity distribution, in order to serve as a rich set of proxies for the fluid flow state. As such, one possible choice would be to use point vortex states
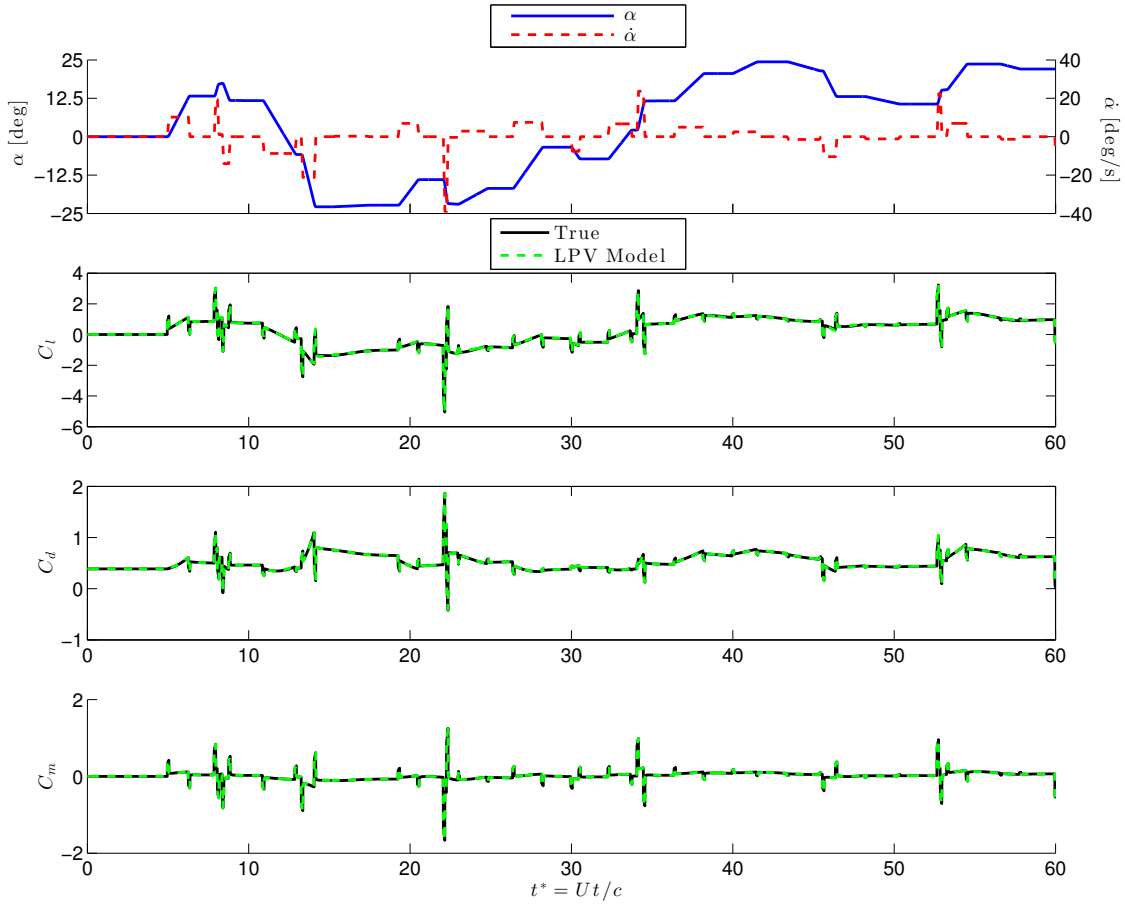
**Figure 4:** Training maneuver moves the airfoil through a wide range of parameter regimes. We identify the three qLPV sub-models based on the "truth" training data generated in numerical simulations for the pseudo-random ramp-hold pitching maneuver with $|\alpha| \le 25°$ shown above. The resulting RMS errors associated with each of identified sub-models for this training maneuver are $\epsilon_{\mathrm{rms}} = 2.3 \times 10^{-2}$ for $C_l$, $\epsilon_{\mathrm{rms}} = 6.2 \times 10^{-2}$ for $C_d$, and $\epsilon_{\mathrm{rms}} = 1.9 \times 10^{-3}$ for $C_m$.

(i.e., position and strength) computed by a low-order point vortex model (e.g., the impulse matching model presented in Wang and Eldredge (2013)) as parameters in a parameter-varying model. In this way, even if the vortex model is only qualitatively accurate, which is the case for most low-dimensional vortex models,[29] the parameters will serve as indicators of the underlying flow physics. Assuming an appropriate selection of parameters, the system identification framework trains the parameter-varying aerodynamic response model with representative input-output data. That is, the model is "tuned" to the given set of parameters in a manner that enables reliable input-output response predictions; hence, qualitative descriptions of the flowfield should be adequate in the context of parameter-varying aerodynamic response modeling, making vortex parameters a feasible candidate for future studies.
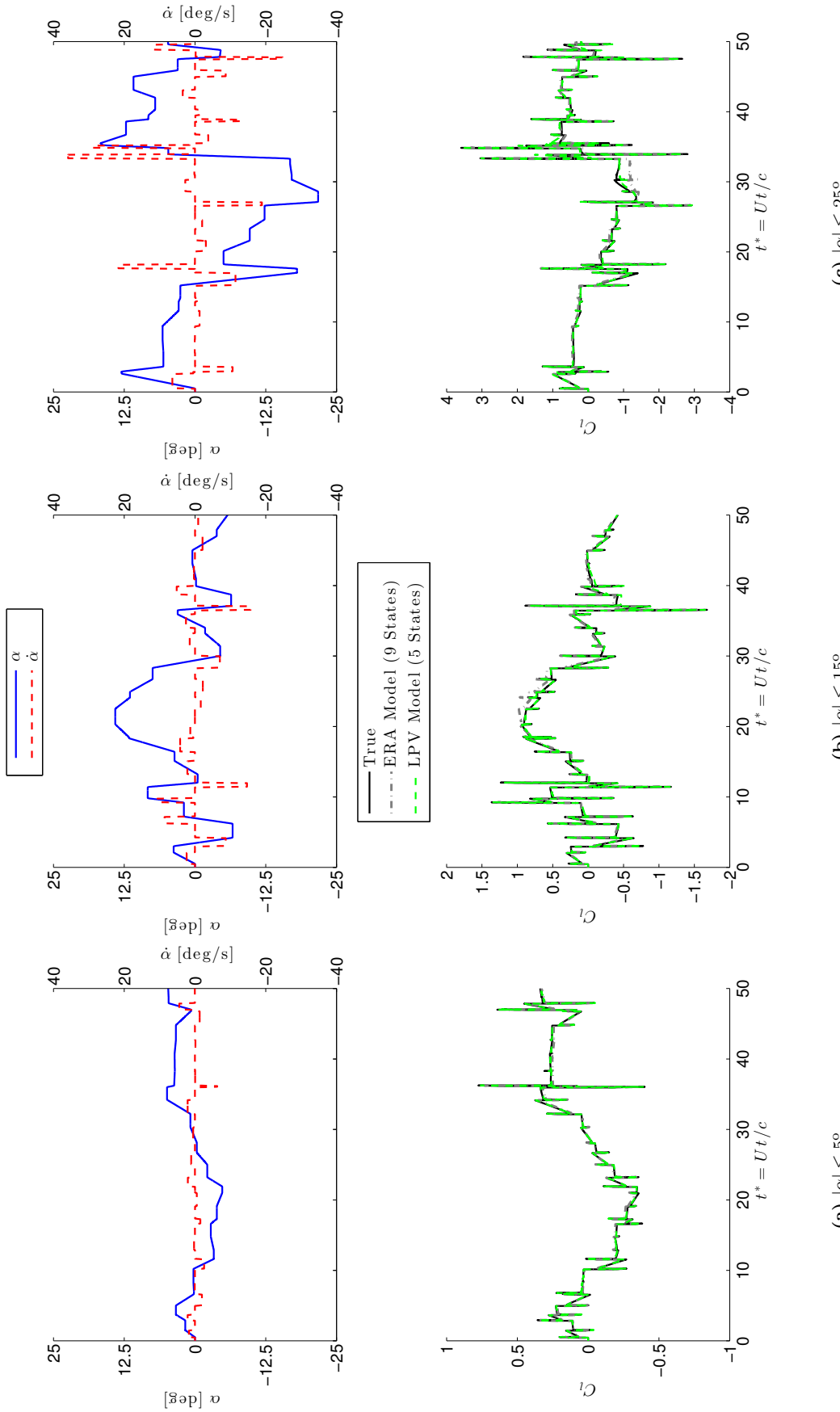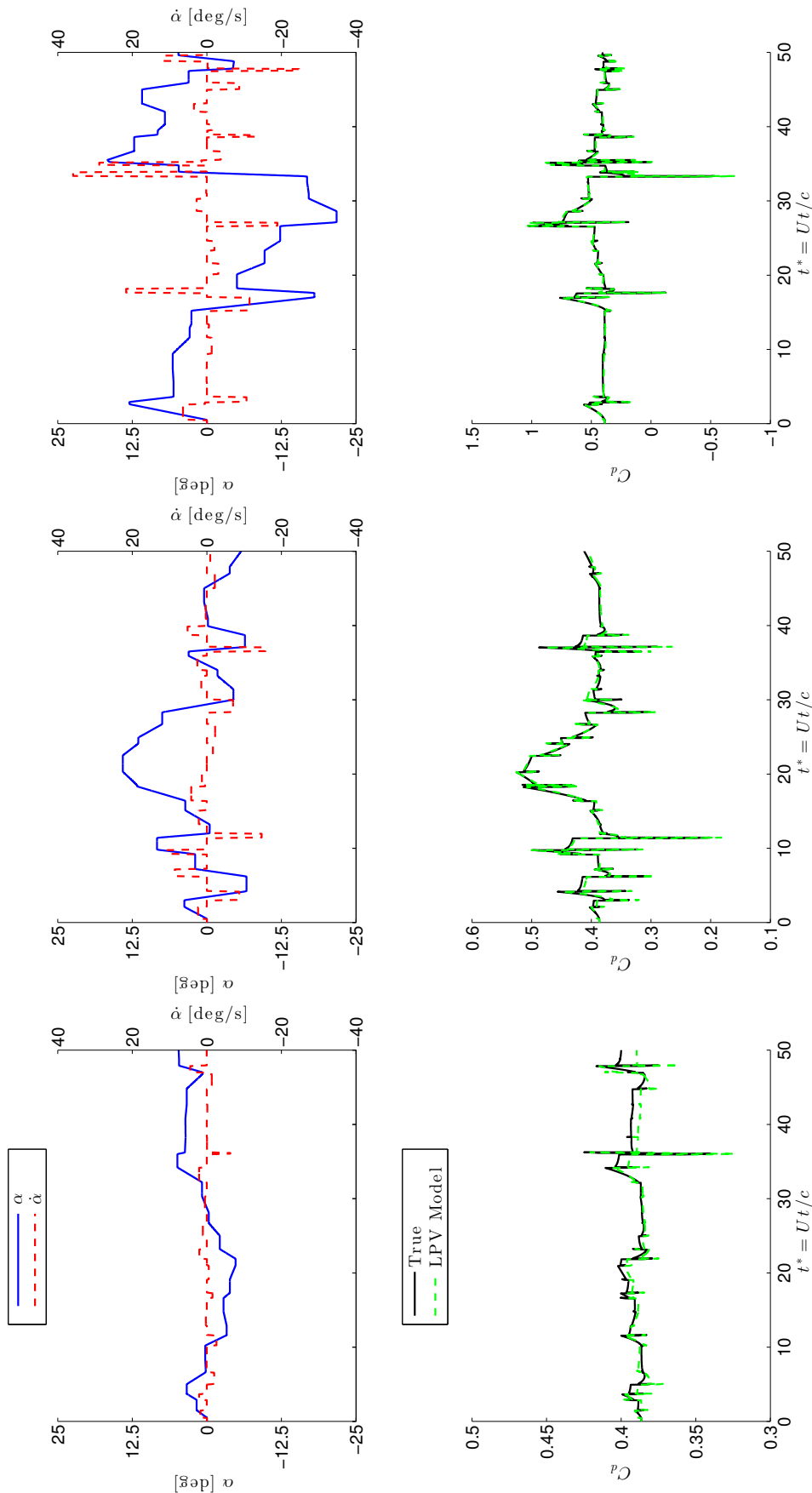
American Institute of Aeronautics and Astronautics

**Figure 5:** Robustness in accuracy of lift predictions from a single identified LPV model. We identify a single LPV model from lift coefficient data corresponding to a pseudo-random ramp-hold pitching maneuver with angle of attack bounded to the range $|\alpha| \leq 25°$. The resulting model is demonstrated on three distinct pseudo-random ramp-hold pitching maneuvers with the following angle of attack bounds (a) $|\alpha| \leq 5°$, (b) $|\alpha| \leq 15°$, and (c) $|\alpha| \leq 25°$. The angle of attack $\alpha$ and its time rate of change $\dot{\alpha}$ associated with a given maneuver are presented in the first row. In the second row, the LPV predicted lift coefficient is plotted in comparison to predictions from a 9-state ERA model as well as the true value computed with IBPM numerical simulations (note the difference in scales for $C_l$ between the different maneuvers). The resulting RMS errors associated with each model for these maneuver sequences are (a) $\epsilon_{rms}^{LPV} = 3.7 \times 10^{-3}$ and $\epsilon_{rms}^{ERA} = 1.5 \times 10^{-2}$, (b) $\epsilon_{rms}^{LPV} = 6.5 \times 10^{-2}$ and $\epsilon_{rms}^{ERA} = 1.4 \times 10^{-1}$, respectively.
$\epsilon_{rms}^{LPV} = 2.1 \times 10^{-2}$ and $\epsilon_{rms}^{ERA} = 2.8 \times 10^{-2}$, and (c) $\epsilon_{rms}^{LPV} = 6.5 \times 10^{-2}$ and $\epsilon_{rms}^{ERA} = 1.4 \times 10^{-1}$, respectively.
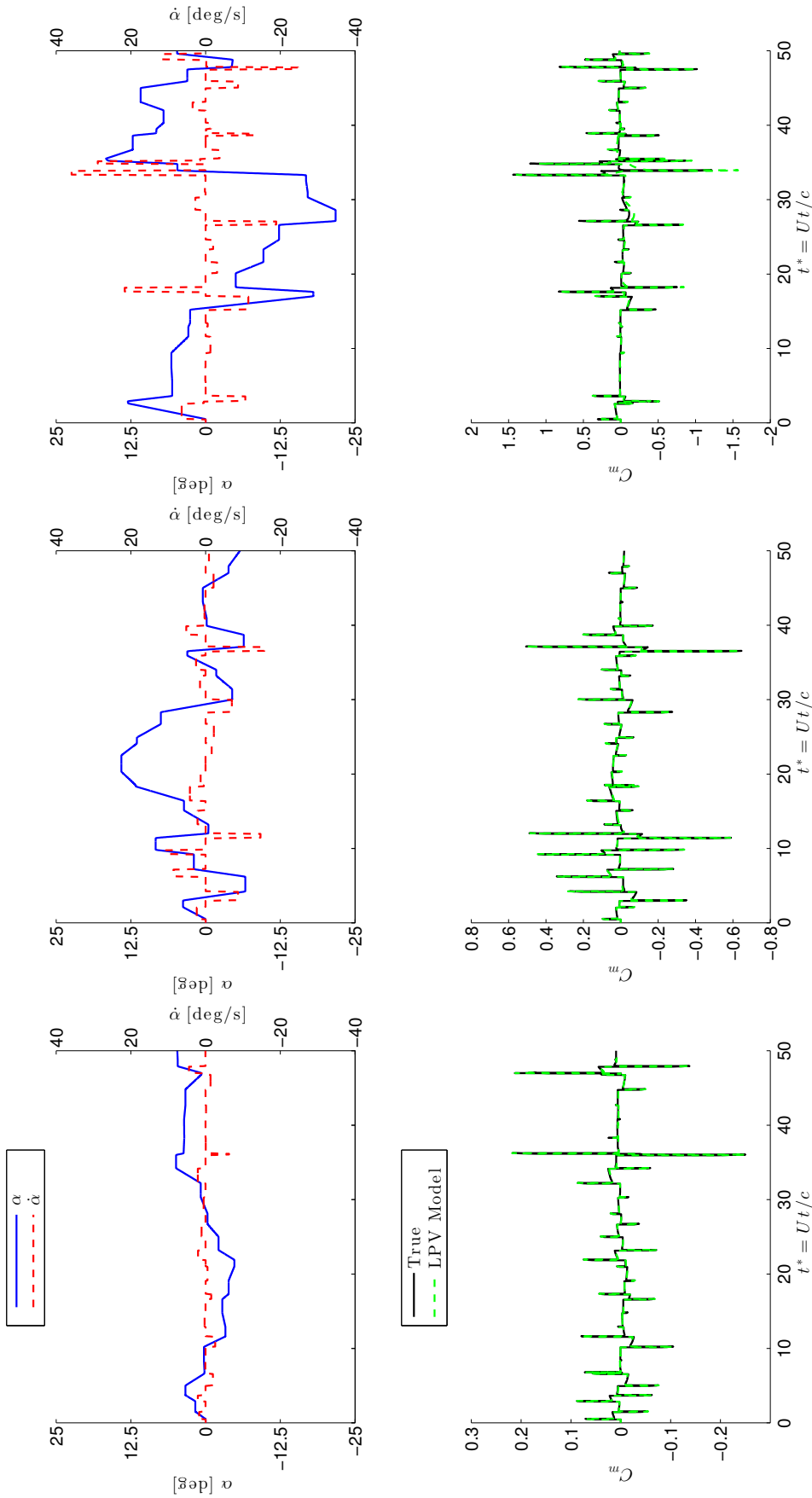
**(a)** $|\alpha| \leq 5^\circ$

**(b)** $|\alpha| \leq 15^\circ$

**(c)** $|\alpha| \leq 25^\circ$

**Figure 6:** Robustness in accuracy of drag predictions from a single identified LPV model. We identify a single LPV model from drag coefficient data corresponding to a pseudo-random ramp-hold pitching maneuver with angle of attack bounded to the range $|\alpha| \leq 25^\circ$. The resulting model is demonstrated on three distinct pseudo-random ramp-hold pitching maneuvers with the following angle of attack bounds (a) $|\alpha| \leq 5^\circ$, (b) $|\alpha| \leq 15^\circ$, and (c) $|\alpha| \leq 25^\circ$. The angle of attack $\alpha$ and its time rate of change $\dot{\alpha}$ associated with a given maneuver are presented in the first row. In the second row, the LPV predicted drag coefficient is plotted in comparison to the true value computed with IBPM numerical simulations (note the difference in scales for $C_d$ between the different maneuvers). The resulting RMS error for each sequence of maneuvers is (a) $\epsilon_{\mathrm{rms}} = 4.3 \times 10^{-3}$, (b) $\epsilon_{\mathrm{rms}} = 4.9 \times 10^{-3}$, and (c) $\epsilon_{\mathrm{rms}} = 1.6 \times 10^{-2}$, respectively.

**(a)** $|\alpha| \leq 5^{\circ}$

**(b)** $|\alpha| \leq 15^{\circ}$

**(c)** $|\alpha| \leq 25^{\circ}$

**Figure 7:** Robustness in accuracy of pitching moment predictions from a single identified LPV model. We identify a single LPV model from pitching moment coefficient data corresponding to a pseudo-random ramp-hold pitching maneuver with angle of attack bounded to the range $|\alpha| \leq 25^{\circ}$. The resulting model is demonstrated on three distinct pseudo-random ramp-hold pitching maneuvers with the following angle of attack bounds (a) $|\alpha| \leq 5^{\circ}$, (b) $|\alpha| \leq 15^{\circ}$, and (c) $|\alpha| \leq 25^{\circ}$. The angle of attack $\alpha$ and its time rate of change $\dot{\alpha}$ associated with a given maneuver are presented in the first row. In the second row, the LPV predicted pitching moment coefficient is plotted in comparison to the true value computed with IBPM numerical simulations (note the difference in scales for $C_m$ between the different maneuvers). The resulting RMS error for each sequence of maneuvers is (a) $\epsilon_{\mathrm{rms}} = 8.5 \times 10^{-4}$, (b) $\epsilon_{\mathrm{rms}} = 2.8 \times 10^{-3}$, and (c) $\epsilon_{\mathrm{rms}} = 4.3 \times 10^{-3}$, respectively.

# VI.    Conclusions

In this study, we formulated a parameter-varying description for the unsteady aerodynamic response of a pitching airfoil based on physical insights gathered from the simulated flowfield from a series of canonical pitch-up maneuvers. We proceeded to frame an output-minimization problem in order to identify a model realization from input-output data, using $(\alpha, \dot{\alpha})$ as model parameters. Numerical experiments indicated that including an additional parameterization by $C_l$ improved predictive performance in the drag response. Based on this observation, we decomposed the full qLPV system into three single-input single-output qLPV sub-models in an effort to make model identification tractable, while allowing for coupling between sub-models. The identified model successfully predicted the force/moment response in a series of "untrained" ramp-hold pitching maneuvers for $|\alpha| \leq 25^\circ$. Comparisons with a linear ERA model highlighted the relevance of non-linear terms in modeling the aerodynamic response in larger amplitude pitch maneuvers. Despite the success in the regime of $|\alpha| \leq 25^\circ$, additional work remains to be conducted to enable reliable predictions at larger angles of attack. One potential means of extending the parameter-varying framework to accommodate such maneuvers is to incorporate parameters computed in a low-order vortex model, in an effort to characterize the qualitative evolution of the flowfield in the identified model.

# VII.    Acknowledgments

# References

[1] H. Wagner, "Über die entstehung des dynamischen auftriebes von tragflügeln," *Zeitschrift für Angewandte Mathematik und Machanik*, vol. 5, no. 1, pp. 17–35, 1925.

[2] T. Theodorsen, "General theory of aerodynamic instability and the mechanism of flutter," Tech. Rep. 496, NACA, 1935.

[3] I. E. Garrick, "Propulsion of a flapping and oscillating airfoil," Tech. Rep. 567, NACA, 1937.

[4] T. von Kármán and W. Sears, "Airfoil theory for non-uniform motion," *Journal of Aeronautical Sciences*, vol. 5, no. 10, pp. 379–390, 1938.

[5] R. Krasny, "Vortex sheet computations: Roll-up, wakes, separation," in *Lectures in Applied Mathematics* (C. R. Anderson, ed.), vol. 28, pp. 385–402, Applied Mathematical Society, 1991.

[6] D. Pullin and Z. Wang, "Unsteady forces on an accelerating plate and application to hovering insect flight," *Journal of Fluid Mechanics*, vol. 509, pp. 1–21, 2004.

[7] M. Jones, "The separated flow of an inviscid fluid around a moving flat plate," *Journal of Fluid Mechanics*, vol. 496, pp. 405–441, 2003.

[8] R. Shukla and J. D. Eldredge, "An inviscid model for vortex shedding from a deforming body," *Theoretical and Computational Fluid Dynamics*, vol. 21, pp. 343–368, 2007.

[9] J. Katz and D. Weihs, "Behavior of vortex wakes from oscillating airfoils," *AIAA Journal*, vol. 15, no. 12, pp. 861–863, 1978.

[10] K. D. Jones, S. J. Duggan, and M. F. Platzer, "Flapping-wing propulsion for a micro air vehicle," in *AIAA Paper 2001-0126*, (Reno, NV), 39th Aerospace Sciences Meeting and Exhibit, January 2001.

[11] S. Ansari, R. Zbikowski, and K. Knowles, "Non-linear unsteady aerodynamic model for insect-like flapping wings in the hover. Part 1: Methodology and analysis," in *Proceedings of IMechE, Part G: Journal of Aerospace Engineering*, vol. 220 (G2), pp. 61–83, 2006.

[12] K. Ramesh, A. Gopalarathnam, J. R. Edwards, M. V. Ol, and K. Granlund, "An unsteady airfoil theory applied to pitching motions validated against experiment and computation," *Theoretical and Computational Fluid Dynamics*, January 2013.

[13] C. Brown and W. Michael, "Effect of leading edge separation on the lift of a delta wing," *Journal of Aeronautical Sciences*, vol. 21, pp. 690–694, 1954.

[14] J. Graham, "The forces on sharp-edged cylinders in oscillatory flow at low Keulegan-Carpenter numbers," *Journal of Fluid Mechanics*, vol. 97, no. 1, pp. 331–346, 1980.

[15] L. Cortelezzi and A. Leonard, "Point vortex model of the unsteady separated flow past a semi-infinite plate with transverse motion," *Fluid Dynamics Research*, vol. 11, pp. 263–295, 1993.

[16] S. Michelin and S. Llewelyn Smith, "An unsteady point vortex method for coupled fluid-solid problems," *Theoretical and Computational Fluid Dynamics*, vol. 23, pp. 127–153, 2009.

[17] C. Wang and J. D. Eldredge, "Low-order phenomenological modeling of leading-edge vortex formation," *Theoretical and Computational Fluid Dynamics*, vol. 27, pp. 577–598, August 2013.

[18] S. L. Brunton, C. W. Rowley, and D. R. Williams, "Reduced-order unsteady aerodynamic models at low Reynolds numbers," *Journal of Fluid Mechanics*, vol. 724, pp. 203–233, 2013.

[19]S. L. Brunton, S. T. Dawson, and C. W. Rowley, "State-space model identification and feedback control of unsteady aerodynamic forces," *Journal of Fluids and Structures*, vol. 50, pp. 253–270, 2014.

[20]R. A. Hyde and K. Glover, "The application of scheduled $H_\infty$ controllers to VSTOL aircraft," *IEEE Transactions on Automatic Control*, vol. 38, pp. 1021–1039, 1993.

[21]R. Nichols, R. Reichert, and W. Rugh, "Gain-scheduling for $H_\infty$ controllers: A flight control example," *IEEE Transactions on Control Systems Technology*, vol. 1, pp. 69–78, 1993.

[22]W. J. Rugh and J. S. Shamma, "Research on gain scheduling," *Automatica*, vol. 36, pp. 1401–1425, 2000.

[23]J. S. Shamma and M. Athans, "Gain scheduling: Potential hazards and possible remedies," *IEEE Control Systems Magazine*, vol. 12, no. 3, pp. 101–107, 1992.

[24]V. Verdult, *"Nonlinear System Identification: A State-Space Approach"*. PhD thesis, University of Twente, 2002.

[25]G. J. Balas, I. Fiahlo, A. Packard, J. Renfrow, and C. Mullaney, "On the design of the LPV controllers for the F-14 aircraft lateral-directional axis during powered approach," in *Proceedings of the American Control Conference*, vol. 1, (Evanston, IL), pp. 123–127, American Automatic Control Council, 1997.

[26]A. Marcos and G. J. Balas, "Development of linear-parameter-varying models for aircraft," *Journal of Guidance, Control, and Dynamics*, vol. 27, pp. 218–228, March-April 2004.

[27]R. Bhattacharya, G. J. Balas, M. A. Kaya, and A. Packard, "Nonlinear receding horizon control of an F-16 aircraft," *Journal of Guidance, Control, and Dynamics*, vol. 25, pp. 924–931, September-October 2002.

[28]M. S. Hemati, *Vortex-Based Aero- and Hydrodynamic Estimation*. PhD thesis, University of California, Los Angeles, 2013.

[29]M. S. Hemati, J. D. Eldredge, and J. L. Speyer, "Improving vortex models via optimal control theory," *Journal of Fluids and Structures*, vol. 49, pp. 91–111, 2014.

[30]T. Johansen and R. Murray-Smith, "The operating regime approach to nonlinear modelling and control," in *Multiple Model Approaches to Modelling and Control* (R. Murray-Smith and T. A. Johansen, eds.), ch. 1, Bristol, PA: Taylor-Francis, 1997.

[31]J. Nocedal and S. J. Wright, *Numerical Optimization*. New York: Springer, 2nd ed., 2006.

[32]L. H. Lee and K. Poolla, "Identifiability issues for parameter-varying and multidimensional linear systems," in *Proceedings of the ASME Design Engineering Technical Conference*, (Sacramento, CA), September 1997.

[33]V. Verdult and M. Verhaegen, "Identification of multivariable LPV state space systems by local gradient search," in *Proceedings of the European Control Conference*, (Porto, Portugal), September 2001.

[34]V. Verdult and M. Verhaegen, "Kernel methods for subspace identification of multivariable LPV and bilinear systems," *Automatica*, vol. 41, no. 9, pp. 1557–1565, 2005.

[35]BILLPV Toolbox, v2.2. http://www.dcsc.tudelft.nl/ datadriven/billpv/, 2010.

[36]K. Taira and T. Colonius, "The immersed boundary method: A projection approach," *Journal of Computational Physics*, vol. 225, no. 2, pp. 2118–2137, 2007.

[37]T. Colonius and K. Taira, "A fast immersed boundary method using a nullspace approach and multi-domain far-field boundary conditions," *Computer Methods in Applied Mechanics and Engineering*, vol. 197, pp. 2131–2146, 2008.